ELSEVIER

Journal of Nuclear Materials 248 (1997) 281–287

journal of nuclear materials

PWR Zircaloy cladding corrosion behavior: quantitative analyses

T. Kido *, K. Kanasugi, M. Sugano, K. Komatsu

Fuel and Material Engineering, Research and Development Department, Nuclear Development Co., 622-12 Hunaishikawa, Tokai-mura, Obaraki-ken 319-11, Japan

Abstract

The causes of accelerated corrosion of Zircaloy-4 fuel cladding at high burnups in PWRs have been reviewed and, among these causes, the effect of hydriding has been investigated using out-of-pile corrosion test results and quantitative analyses. The review shows that the lithium effect and the microstructural change of Zircaloy-4 have potential to accelerate the corrosion rate. However, consistent data base applicable to quantitative analyses of PWR corrosion is not enough. On the other hand, the out-of-pile corrosion data shows that hydriding could accelerate the corrosion rate by a factor of up to 4. A new corrosion model which can take account of hydrogen movement showed hydriding is a plausible factor to determine the high burnup corrosion behavior. © 1997 Elsevier Science B.V.

1. Introduction

Among numerous works on the corrosion behavior of Zr-base alloys, one of the most important aspects is to elucidate the cause of accelerated uniform corrosion of Zircaloy-4 cladding at high burnup in PWRs.

The phenomenon of accelerated corrosion has become clear as the extended burnup corrosion data from PWRs accumulates. Based on test results, the tin content of Zircaloy-4 has been reduced in an attempt to minimize the rate of corrosion. This, so called low-tin-content Zircaloy-4, has become an industrial standard and is widely utilized in LWR's at present. The corrosion behavior of low-tin Zircaloy-4 cladding is shown in Fig. 1 [1–4]. The trend shown in Fig. 1 are not fully correct from the view point of corrosion consideration since the horizontal axis of Fig. 1 is given in burnup and factors affecting corrosion rate such as the temperature histories and water chemistry, are not taken into account. The effectiveness of reducing the tin content on the retarding corrosion rate is expected to be confirmed more precisely in the near future as in-reactor data of this type of Zircaloy-4 is accumulated. However, it is useful to gather provisional corrosion data from the literature in the meantime. As shown in Fig. 1, the low-tin Zircaloy-4 cladding follows a similar trend to that of the conventional-tin-content Zircaloy-4 cladding, i.e., corrosion is accelerated at high burnup. Moreover, reduced scatter of the data and a clearer transition point from the incubation period to the accelerated corrosion regime are seen in comparison with conventional-tin-content Zircaloy-4. This is probably due to reduced variation in tin content. On the other hand, the oxide thickness from which the acceleration occurs remains approximately 10 to 20 μm and does not change from the tendency of the conventional-tin-content Zircaloy-4 cladding. The slopes of oxide growth against burnup accumulation before and after the onset of corrosion acceleration differs by a factor of four as illustrated by the dashed lines in Fig. 1.

Since the above-mentioned provisional data shows accelerated corrosion at high burnup is also observed for low-tin Zircaloy-4 cladding, it may be useful to continue clarifying factors which have been reported as the plausible causes of the acceleration. In addition to mechanistic consideration, quantitative analysis on the causes is recommended to see which cause is dominant.

This paper reviews the literature with respect to quantitative data on the possible causes first. Secondly the effect of hydriding on corrosion, which is shown to be one of the

* Corresponding author. Tel.: +81-29 282 9594; fax: +81-29 287 0889; e-mail: kido@ndcgw.hq.mhi.co.jp.

PII S0022-3115(97)00125-6

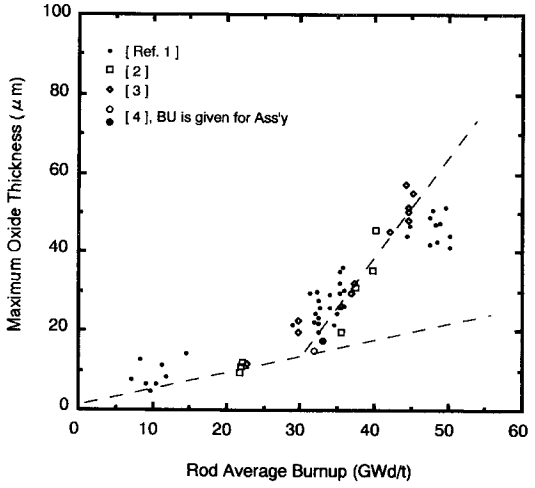

Fig. 1. Maximum oxide thickness of low tin cladding as a function of rod average burnup.

possible causes by reviewing, is discussed based on the results of our out-of-pile corrosion experiments.

2. Literature review

The hypotheses for the cause of accelerated uniform corrosion at high burnup in PWRs might be categorized as follows.

(1) Thermal conductivity degradation of the ZrO_2 as the oxide thickens [5].

(2) Loss of corrosion resistance of Zircaloy matrix brought by changes in the microchemistry due to the irradiation [6].

(3) Accumulation of lithium in the ZrO_2 and loss of the protective nature of the oxide at the metal–oxide interface [7,8].

(4) Build up of the isolated water chemistry in the oxide of thicker than 12 μm (thick-film effect) [9].

(5) Deleterious effect on corrosion of the formation and/or presence of zirconium-hydride [10,11].

2.1. Thermal conductivity degradation of the oxide

Two factors which affect the thermal conductivity of the oxide are; the accumulation of the irradiation damage and change in the density of the oxide. The results from measurements on the oxide irradiated in PWRs are insufficient. The only data set available is shown in Fig. 2 which allows us to assess the effect of irradiation and of oxide thickness [5]. The thermal conductivity of the irradiated oxides is in the range 1.5 to 2.0 W/m K. The thickest oxide gives the lowest value and the smallest scatter. If one assumes that the thermal conductivity of the irradiated oxide starts from 2.0 W/m K, a reduction of approximately 30% is observed. This reduction in the thermal conductivity of the oxide can cause an increase in temperature of approximately 5 K in the metal-oxide interface for a 50 μm oxide at linear heat rate of 20 kW/m. This corresponds to approximately 20% acceleration in the post-transition corrosion rate with typical activation energy [12]. The extent of this effect is not large enough to explain the accelerated corrosion completely and few corrosion models have utilized this effect. A further concern about this factor is the possibility of further degradation of the oxide thermal conductivity during operation due to the formation of steam phase in the pore or cracks of the oxide.

2.2. Changes in the microchemistry

In the last decade, the relationship between the distribution of the intermetallic particles and the in-reactor corrosion behavior has been well established. The investigations [13,14] have confirmed that the appropriate size distribution of the intermetallic particles exists to give good in-reactor corrosion performance. On the other hand, the re-dissolution of the intermetallic particles due to irradiation has been shown to have an influence on the corrosion resistance of the materials irradiated in BWR [6].

Fig. 3 is an example showing the effect of irradiation on the post-irradiation corrosion [6]. The corrosion rates of the irradiated base materials in 673 K steam are clearly increased by a factor of approximately four compared to that of the unirradiated materials. The extent of this increase in the corrosion rate is adequate to account for the in-reactor behavior. However, the materials tested have been irradiated in BWR and are therefore irradiated at lower temperature than would be the case for PWR claddings. Since the dissolution phenomenon is reported to be temperature-dependent [15] and is enhanced at lower temperature, one should be careful to apply these results to

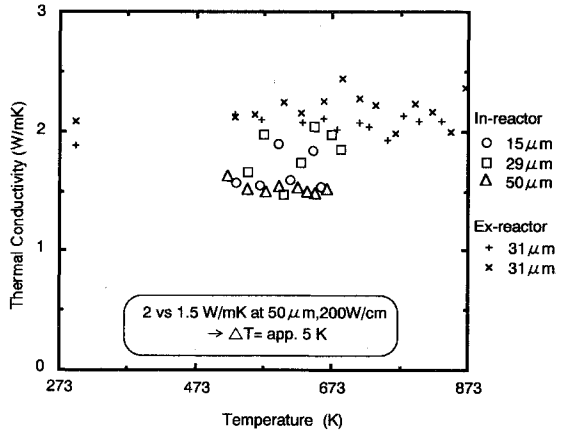

Fig. 2. Thermal conductivity of the oxide on irradiated cladding materials [5].

PWR materials immediately. Temperature in the cladding with oxide of more than 60 μm is approximately 633 K during operation. Around this temperature level, the dissolution of the intermetallic particles is reported to be replaced by ripening [16]. Since the effect of particle ripening may improve corrosion resistance, the rate of corrosion should be decreased in the region where the oxide thickness exceeds about 60 μm. However, declining tendency of the accelerated corrosion has not observed clearly [1–3,17].

In order to clarify the effect of the microstructural change on the corrosion behavior of PWR cladding, more investigations, especially post-irradiation corrosion tests coupled with microstructural examinations, are required.

2.3. Accumulation of lithium in the oxide

The influence of lithium on the corrosion property of Zircaloy has been investigated for more than thirty years [7,8,18–21], mainly by means of out-of-pile corrosion tests. However, the effect of lithium on the in-pile corrosion is ambiguous. Because in-pile data are only available from in-reactor demonstrations of the high lithium operation in the commercial reactors except one investigation performed in the Halden reactor [22–24]. These data include many valuables which should be taken into account and make it difficult to quantify the effect of lithium on the in-reactor corrosion of the cladding.

Although there is still much argument about the determining factor of the lithium effect, a correlation between the corrosion rate and the concentration of lithium in the formed oxide seems to shows good agreement. The lithium concentration in the oxide from which the corrosion is accelerated has settled somewhere between 50 to 100 ppm by weight according to the out-of-pile corrosion data [7,19].

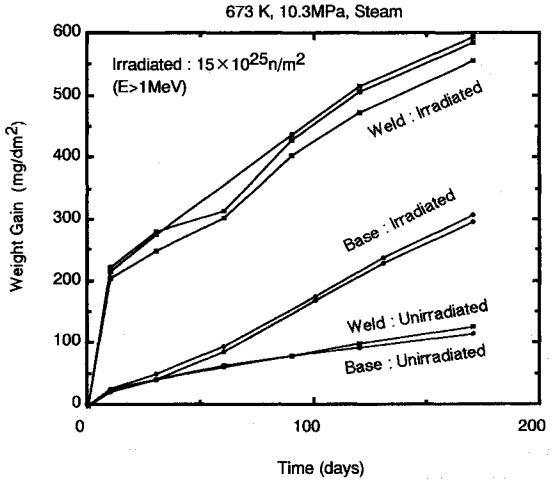

Fig. 3. Post-irradiation corrosion test results on Zircaloy-4 channels irradiated in BWR [6].

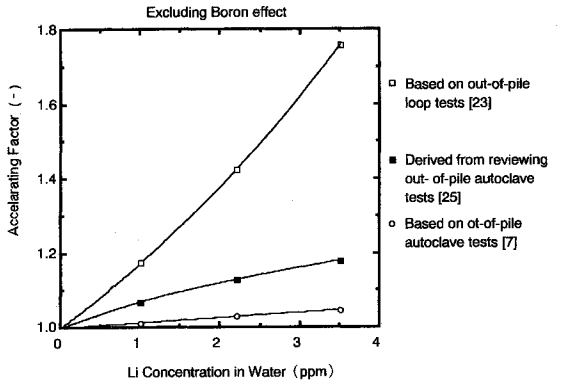

Fig. 4. Calculated data to demonstrate lithium effect on the corrosion rate.

There are no in-reactor data which enable us to directly compare the lithium concentration in the oxide with the corresponding corrosion rate. Only empirical models expressing the relation between the lithium concentration in water and the acceleration factor for the corrosion rate are available. Fig. 4 summarizes the effect of lithium derived by these models [7,23,25]. Although one of the models shows good predictability for the accelerated corrosion at high burnup [25], inconsistency in the extent of this effect is relatively large as shown in Fig. 4. And there is insufficient data to link the extent of the acceleration to the knowledge established by the ex-reactor materials, for example, the lithium depth profile or changes in the lithium concentration or in the irradiated oxides as a function of time. In order to fill this gap additional in-pile as well as out-of-pile data are required.

2.4. Thick film effect

This hypothesis is based on two experimental results: (1) the Zircaloy corrosion is enhanced by the synergistic effect of radiation and oxygenated water [26], (2) the corrosion rate on the samples with thick oxides (> 12 μm) is accelerated irrespective of the water chemistry during irradiation [11]. These observations lead to the conclusion: beyond a threshold oxide thickness the water chemistry inside the oxide is isolated from the bulk water and controls the corrosion rate.

Although the hypothesis is well explained [11], the corrosion rate under onset of this effect is reported around 2.0 mg/dm^2 day at temperature of 553 to 563 K. This seems too large because an expected corrosion rate on the ordinary Zircaloy may be less than one twentieth. In order to confirm the effectiveness of this effect, some experiments under conditions similar to PWR are necessary.

2.5. Hydriding

The first trial to explain the enhanced corrosion at high burnup in PWRs with the effect of hydride precipitation was conducted by Garde [10]. Before that the corrosion rate transition attributed to hydriding was reported by Cox [27], but hydrogen concentration at which the acceleration occurred was about 1500 to 2000 ppm and seemed too high to be applied to the enhanced corrosion in PWRs. This was probably due to the high corrosion temperature (773 K). Other data have been presented recently by Blat et al. by means of out-of-pile corrosion tests on samples pre-hydrided by gaseous and cathodic charging in steam at 673 K [28]. Their results have shown that the influence of massive hydride layer seems dominant. Along with these ex-reactor data, enhanced oxide thicknesses have been detected on the irradiated materials where the hydride heavily precipitated [29,30].

Although the effect of hydriding on the corrosion behavior has been analyzed quantitatively [11,31], there are little data on the temperature dependence of this effect. Therefore, we have performed long-term out-of-pile corrosion tests to quantify the temperature dependence of the effect of hydriding on the corrosion rate of Zircaloy-4.

3. Assessment on hydriding effect by out-of-pile corrosion tests

3.1. Experimental

In an attempt to quantify the effect of hydriding on the corrosion rate, the samples (pre-hydrided) were subjected to long-term out-of-pile corrosion tests.

A Zircaloy-4 tube lot of PWR fuel cladding geometry was selected for corrosion tests. Concentrations of major elements are shown in Table 1. The accumulated annealing parameter of the tube was typical for PWR materials. The final tube heat treatment was stress relief annealing.

Charging of hydrogen to the samples prior to conducting corrosion test was done by exposing 150 mm long samples to a hydrogen/argon gas mixture at about 673 K. Exposure time and hydrogen/argon ratio were varied so that with several levels of hydrogen concentration were obtained. The surface of the as-received sample was mechanically abraded. After hydrogen charging, the sample was cut into 10 mm long tubes and every tube-end was analyzed for hydrogen concentration determination.

Table 1
Chemical composition of Zircaloy-4 used for corrosion tests

Element	Unit	Range	Average
Sn	wt%	1.54–1.58	1.55
Fe	wt%	0.20–0.22	0.21
Cr	wt%	0.10–0.11	0.11
C	ppm	120–140	130
Si	ppm	94–105	102
H [a]	ppm	7–8	8
N [a]	ppm	29–30	30
O [a]	ppm	1230–1250	1240

[a] Measurements of the cladding.

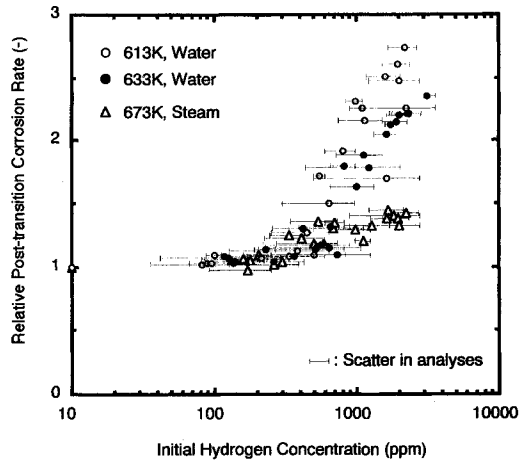

Fig. 5. Effect of initial hydrogen concentration on post-transition corrosion rate.

Corrosion tests were conducted in deionized water at 613 and 633 K, 19 MPa in a refreshed autoclave and in steam at 673 K, 10.3 MPa in a static autoclave. The level of dissolved oxygen in the water in the refreshed autoclaves was maintained at less than 5 ppb by hydrogen overpressure. This resulted in a dissolved hydrogen level of 10 to 20 $cm^3/kg\ H_2O$. Five 10 mm long samples from the original tube were loaded into each autoclave as control material together with the pre-hydrided samples. The samples were weighed after each 30-day autoclave cycle for the weight gain calculation. The total exposure times were 398 and 210 days for the samples corroded in water and steam, respectively. Selected samples were subjected to hydrogen analysis after completion of the corrosion tests.

3.2. Results

Fig. 5 shows the results of the corrosion test in the form of a relationship between initial hydrogen concentration and post-transition corrosion rate. The initial hydrogen concentrations of the starting materials were up in excess of 3000 ppm as a result of hydrogen charging. The post-transition corrosion rate on each sample was derived by a least-square fit of the weight gain data with exposure time after the transition point at each corrosion test temperature and was normalized to the average corrosion rate of as-received samples. As clearly shown in Fig. 5, the corrosion rates in water at 613 and 633 K were accelerated for the

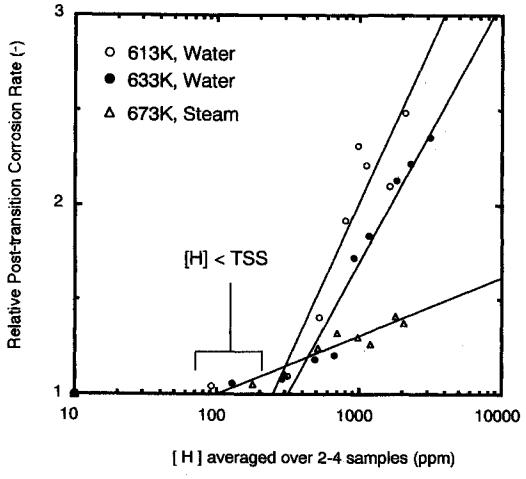

Fig. 6. Effect of initial hydrogen concentration on post-transition corrosion rate (2).

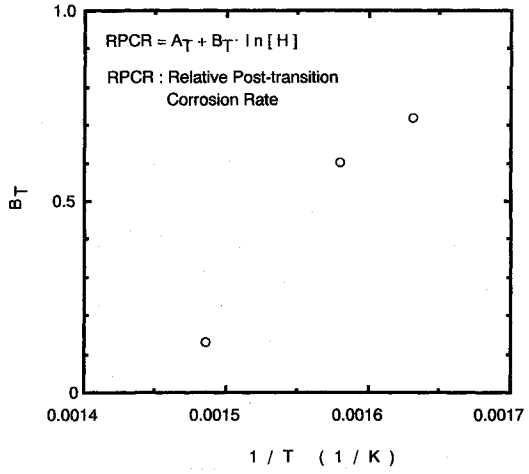

Fig. 7. Arrhenius plot of acceleration factor for post-transition corrosion rate.

samples with higher initial hydrogen levels. Conversely, the corrosion rates on the samples with similar level of hydrogen show only slight increase in corrosion rate in steam at 673 K. Although it was not so clear due to relatively large scatter in the initial hydrogen concentration of the samples, the accelerated phenomenon became obvious when the sample contained more than 200 to 400 ppm of hydrogen.

In order to simplify the results shown in Fig. 5, the individual data were averaged over two to four samples with similar hydrogen concentrations as shown in Fig. 6. Fig. 6 shows that the acceleration of corrosion increases with decreasing temperature. With respect to the tests in water, the rate of corrosion was greater for lower hydrogen concentration at 613 K than at 633 K. The results in steam at 673 K showed that corrosion was accelerated from the lowest hydrogen concentration though the extent of acceleration was small. The samples with hydrogen concentrations slightly less than the hydrogen terminal solid solubility (presented by 'TSS' in Fig. 6) showed a slight increases in corrosion rate at each test temperature. Since hydride precipitation is attended with the volume expansion and is thought to be a cause to damage the oxide, these samples were loaded in the autoclaves so that the effect of the onset of hydride precipitation on corrosion could be investigated. The results show that hydride precipitation has little effect on the acceleration of corrosion. It may be considered that the presence of hydride has more significant effect than the precipitation of hydride.

The extent of acceleration was evaluated for the data with a hydrogen concentration above 200 ppm and is expressed by the following equation:

$$\mathrm{RPCR} = A_T + B_T \ln[\mathrm{H}], \quad (1)$$

where RPCR is the relative post-transition corrosion rate, A_T and B_T are constants at temperature T and [H] is the hydrogen concentration in ppm. The temperature dependency of evaluated B_T is shown in Fig. 7.

The hydrogen absorption fraction was calculated by means of the weight gain data and the results from hydrogen analysis and is plotted in Fig. 8. Due to the variation in the initial hydrogen level of each sample, the scatter bands are quite large. It is difficult to assess the effect of hydriding on the hydrogen absorption property at present.

3.3. Discussion

From the experimental results represented in Section 2.5, the potential of hydriding to be a cause of the accelerated corrosion is well supported. In order to determine the applicability of this effect with respect to high burnup corrosion of the PWR cladding, analysis accounts for

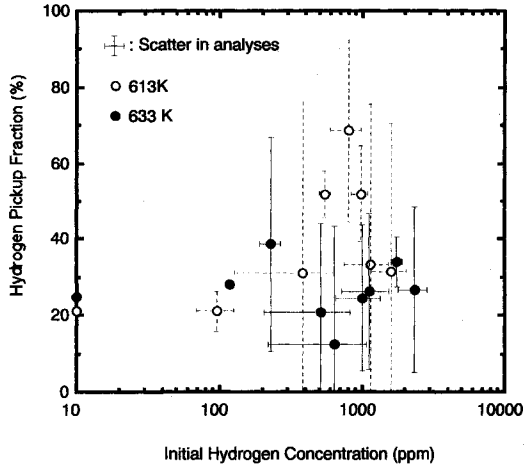

Fig. 8. Effect of initial hydrogen concentration on hydrogen pickup at 387 days exposure.

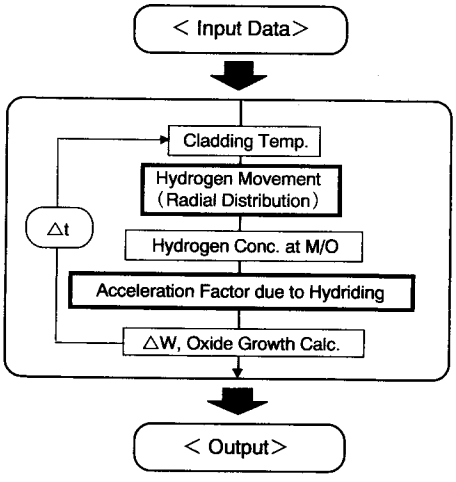

Fig. 9. Flow chart of the corrosion model.

hydrogen movement in the cladding because hydride precipitation occurs first at the colder outside surface (metal-oxide interface) under heat flux conditions and corrosion initiates in the same position.

For this purpose, we have developed a corrosion model coupled with a model of hydrogen movement [11]. A flow chart of the corrosion model is shown in Fig. 9. The acceleration factor in the model is based on the results of the out-of-pile corrosion data given in Section 3.2. Hydrogen concentration at which acceleration due to hydriding becomes active is settled to 200 ppm referring to the scatter of the data shown in Fig. 5.

Examples calculated by the model are given in Fig. 10. In Fig. 10, a comparison of the predictions with and without the acceleration effect are shown. Detailed description of the fundamental corrosion model and constants are given in Ref. [11]. The calculation has been made for an axial position of cladding where corrosion is most severe under typical PWR conditions. The model predictions realized two features which were in a reasonable agreement with a comprehensive trend of in-PWR corrosion data similar to that shown in Fig. 1. First, the second transition point is obvious at the oxide thickness of 15 μm. Second, the deviation from the conventional calculation result was obvious after approximately 30 GW d/t irradiation after passing the second transition point. Consequently, the hydrogen buildup at the outer surface of the fuel cladding may be hypothesized to be one of the possible causes of the corrosion enhancement at high burnups.

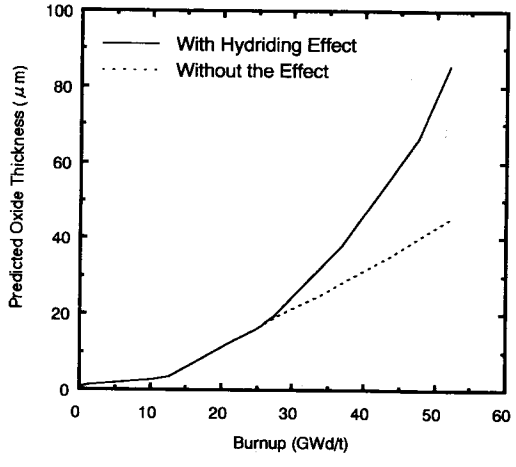

Fig. 10. Predicted oxide thickness as a function of burnup for typical PWR fuel cladding.

In the present model and calculations, however, neither irradiation effect nor lithium effect on the influence of hydriding are taken into account. These effects are thought to be other plausible factors for the accelerated corrosion as discussed in Section 2. In order to confirm any synergistic effects of these factors, further experiments especially under irradiation are still needed.

4. Conclusions

The causes of enhanced corrosion of Zircaloy-4 fuel cladding at high burnups in PWRs have been reviewed and, among these causes, the effect of hydriding on the corrosion has been investigated.

A review of the literature showed changes in the microchemistry of Zircaloy-4 matrix due to irradiation and accumulation of lithium into the oxide may have significant effects on the corrosion rate. Additional data is needed for confirmation, especially for consideration under PWR conditions.

Out-of-pile corrosion tests with pre-hydrided Zircaloy-4 samples have made it possible to establish a relationship between hydrogen concentration and the corrosion rate of Zircaloy-4. A corrosion model which can take account of hydrogen movement has been developed. Calculations with the model showed hydriding is a plausible factor to determine the high burnup corrosion behavior.

Acknowledgements

The authors are grateful to the following colleagues at Nuclear Development Corp. for different tasks: Y. Yamaguchi and H. Nonaka (autoclave testing and data reduction), S. Seino (developing the model) and K. Murai. The authors also express their thanks to H. Kubo, T. Takahashi and S. Doi at Mitsubishi Heavy Industries, Ltd. for useful discussions. This study was funded by Mitsubishi Heavy Industries.

References

[1] M. Limback, M.A. Krammen, P. Rudling, S.R. Pati, A.M. Garde, Proc. ANS Int. Topical Meeting on Light Water Reactor Fuel Performance, West Palm Beach, FL, USA, Apr. 17–21, 1994, pp. 286–295.

[2] G.P. Sabol, W.J. Leech, R.A. Weiner, R.S. Miller, Proc. EPRI, Utility Workshop on PWR Fuel Corrosion, Washington DC, USA, July 28–30, 1993.

[3] O.A. Besch et al., 11th Int. Symp. on Zirconium in the Nuclear Industry, Garmisch-Partenkirchen, Germany, Sept. 11–14, 1995.

[4] H. Hayashi, T. Okubo, Enlarged Halden Programme Group Meeting, Loen, Norway, May 19–24, 1996.

[5] H. Stehle, F. Garzarolli, A.M. Garde, P.G. Smerd, ASTM STP 824 (ASTM, Philadelphia, PA, 1984) pp. 483–506.

[6] B. Cheng, R.M. Kruger, R.B. Adamson, ASTM STP 1245 (ASTM, Philadelphia, PA, 1994) pp. 400–418.

[7] S.G. McDonald, G.P. Sabol and K.D. Sheppard, ASTM STP 824 (ASTM, Philadelphia, PA, 1984) pp. 519–530.

[8] D. Pecheur, J. Godlewski, P. Billot, J. Thomazet, ASTM STP 1295 (ASTM, Philadelphia, PA, 1996) pp. 94–113.

[9] A.B. Johnson Jr., PNL-SA-17065, Proc. IAEA Technical Committee Meeting on Fundamental Aspects of Corrosion of Zirconium-Based Alloys in Water Reactor Environments, Portland, Oregon, USA, Sept. 11–15, 1989.

[10] A.M. Garde, ASTM STP 1132 (ASTM, Philadelphia, PA, 1991) pp. 566–594.

[11] T. Kido, Proc. 6th Int. Symp. on Environmental Degradation of Materials in Nuclear Power Systems, Water Reactors, San Diego, CA, USA, Aug. 1–5, 1993.

[12] F. Garzarolli, D. Jorde, R. Manzel, G.W. Parry, P.G. Smerd, EPRI NP-1472, 1980.

[13] F. Garzarolli, P.G. Smerd, IAEA Int. Symp. on Improvements in Water Reactor Fuel Technology and Utilization, Stockholm, Sept. 15–19, 1986.

[14] F. Garzarolli, R. Schumann, E. Steinberg, ASTM STP 1245 (ASTM, Philadelphia, PA, 1994) pp. 709–723.

[15] A.T. Motta, F. Lefebvre, C. Lemaignan, ASTM STP 1132 (ASTM, Philadelphia, PA, 1991) pp. 718–739.

[16] F. Garzarolli, R. Manzel, F. Sontheimer, Workshop on Zircaloy Corrosion and Hydriding, Halden, Norway, Oct. 15, 1993.

[17] L.F. van Swam, F. Garzarolli, E. Steinberg, Advanced PWR Cladding, Proc. ANS Int. Topical Meeting on Light Water Reactor Fuel Performance, West Palm Beach, Florida, Apr. 17–21, 1994, pp. 303–308.

[18] H. Coriou, L. Grall, J. Meuneier, M. Pelras, H. Willermoz, J. Nucl. Mater. 7 (3) (1962) 320.

[19] F. Garzarolli, J. Pohlmeyer, S. Trapp-Pritsching, H.G. Weidinger, Proc. IAEA Technical Committee Meeting on Fundamental Aspects of Corrosion of Zirconium-Based Alloys in Water Reactor Environments, Portland, Oregon, USA, Sept. 11–15, 1989.

[20] I.L. Bramwell, P.D. Parsons, D.R. Tice, ASTM STP 1132 (ASTM, Philadelphia, PA, 1991) pp. 628–642.

[21] N.Ramasubramanian, P.V. Balakrishnan, ASTM STP 1245 (ASTM, Philadelphia, PA, 1994) pp. 378–399.

[22] B. Cheng, EPRI PWR Plant Chemists Meeting, San Diego, 1992.

[23] D. Pecheur, A. Giordano, E. Picard, Ph. Billot, J. Thomazet, Proc. IAEA Technical Committee Meeting on Influence of Water Chemistry on Fuel Cladding Behaviour, Rez, Czech Republic, Oct. 4–8, 1993.

[24] T. Karlsen, C. Vitanza, ASTM STP 1245 (ASTM, Philadelphia, PA, 1994) pp. 779–789.

[25] Nuclear Electric, A Comparison of Zircaloy Oxide Thicknesses on Millstone-3 and North Anna-1 PWR Fuel Cladding, EPRI TR-102826, Aug. 1993.

[26] A.B. Johnson Jr., J.E. LeSurf, R.A. Proebstle, ASTM STP 551 (ASTM, Philadelphia, PA, 1974) pp. 495–513.

[27] B. Cox, Corrosion 18 (1962) 33t.

[28] M. Blat, D. Noel, ASTM STP 1295 (ASTM, Philadelphia, PA, 1996) pp. 319–337.

[29] G.P. Smith Jr., Proc. EPRI, Utility Workshop on PWR FuelCorrosion, Washington, DC, July 28–30, 1993.

[30] Y.S. Kim, K. S. Rheem, D. K. Min, ASTM STP 1245 (ASTM, Philadelphia, PA, 1994) pp. 745–759.

[31] B. Cheng, P.M. Gilmore, H.H. Klepfer, ASTM STP 1295 (ASTM, Philadelphia, PA, 1996) pp. 137–160.